Ages and growth rates of some deep-sea gorgonian and antipatharian corals of Newfoundland and Labrador

Owen A. Sherwood and Evan N. Edinger

Abstract: Using bomb-^{14}C dating and growth ring counting methods, we calculate life spans and growth rates of six species of deep-sea corals collected at depths of between 400 and 900 m from the continental slope of Newfoundland and Labrador. Bamboo corals (*Acanella arbuscula*, *Keratoisis ornata*) and antipatharians (*Stauropathes arctica*) secrete concentric growth rings in their axial skeletons, which were proven to form annually for *K. ornata* and *S. arctica*. These species had the lowest radial growth rates of 33 ± 11 to 75 ± 11 μm·year^{-1}. *Primnoa resedaeformis* and *Paramuricea* spp. had higher radial growth rates of 83 ± 6 to 215 ± 37 μm·year^{-1}. *Paragorgia arborea* had the highest radial growth rate of 830 ± 120 μm·year^{-1}. Axial growth rates ranged from 0.56 ± 0.05 cm·year^{-1} for a specimen of *Paramuricea* spp. to 2.61 ± 0.45 cm·year^{-1} for a specimen of *Primnoa resedaeformis*. Life spans ranged from 18 ± 4 years for a live-collected *P. resedaeformis* to 200 ± 30 years for a subfossil specimen of *K. ornata*. Because all of the corals were from heavily fished areas, it is likely that age distributions are biased towards smaller and younger colonies. Recovery of deep-sea corals from fishing-induced damage will take decades to centuries.

Résumé : L'utilisation de méthodes de datation basées sur le ^{14}C des essais nucléaires et le dénombrement des anneaux de croissance nous a permis de déterminer la durée de vie et les taux de croissance de six espèces de coraux marins d'eau profonde récoltées sur la pente continentale de Terre-Neuve et du Labrador, à des profondeurs de 400 m à 900 m. Les coraux bambous (*Acanella arbuscula*, *Keratoisis ornata*) et antipathariens (*Stauropathes arctica*) sécrètent des anneaux de croissance concentriques sur leur squelette axial et il est démontré que chez *K. ornata* et *S. arctica* ces anneaux se forment annuellement. Ces espèces possèdent les taux de croissance radiale les plus bas, de 33 ± 11 μm·an^{-1} à 75 ± 11 μm·an^{-1}. *Primnoa resedaeformis* et *Paramuricea* spp. ont des taux de croissance radiale plus élevés, 83 ± 6 μm·an^{-1} à 215 ± 37 μm·an^{-1}. *Paragorgia arborea* présente le taux de croissance radiale le plus élevé, 830 ± 120 μm·an^{-1}. Les taux de croissance axiale varient de 0,56 ± 0,05 cm·an^{-1} chez un spécimen de *Paramuricea* spp. à 2,61 ± 0,45 cm·an^{-1} chez un spécimen de *P. resedaeformis*. Les durées de vie vont de 18 ± 4 années chez un *P. resedaeformis* récolté vivant à 200 ± 30 ans pour un spécimen subfossile de *K. ornata*. Puisque tous les coraux proviennent de régions soumises à une pêche intensive, il est vraisemblable que les distributions d'âge favorisent les colonies plus petites et plus jeunes. La récupération des coraux marins d'eau profonde des dommages infligés par la pêche prendra des décennies et même des siècles.

[Traduit par la Rédaction]

Introduction

In recent years there has been increasing interest in the ecology and biology of deep-sea or cold-water coral ecosystems (Freiwald and Roberts 2005; Roberts et al. 2006). Off eastern Canada, deep-sea coral ecosystems comprise gorgonian and antipatharian "coral forests" located predominantly along the upper continental slope at depths of between 200 and 1000 m (Gass and Willison 2005; Mortensen et al. 2006; Wareham and Edinger 2007). These structurally complex ecosystems support a diversity of associated invertebrates and fish (Krieger and Wing 2002; Stone 2006; Edinger et al. 2007*a*). Deep-sea corals are highly vulnerable to the impacts of bottom trawling (Koslow et al. 2001; Hall-Spencer et al. 2002; Edinger et al. 2007*b*). Unfortunately, widespread industrialization of fishing fleets off eastern Canada and in other regions predates much of the recent scientific interest in deep-sea corals. As a result, trawling impacts to coral habitats may have gone on virtually unnoticed for decades (Haedrich et al. 2001; Kulka and Pitcher 2002).

Information on growth rates and life spans of deep-sea corals is important for their conservation and management. These parameters are vital for assessing the vulnerability of these organisms to natural and anthropogenic disturbances and the time scale of their recovery. One of the dominant gorgonian species off eastern Canada, *Primnoa resedaeformis*, is known to live for at least 700 years (Sherwood et al.

Received 26 March 2008. Accepted 21 September 2008. Published on the NRC Research Press Web site at cjfas.nrc.ca on 23 January 2009.
J20482

O.A. Sherwood.[1] Department of Biology, Memorial University of Newfoundland. St. John's, NL A1B 3X9, Canada.
E.N. Edinger. Departments of Biology and Geography, Memorial University of Newfoundland, St. John's, NL A1B 3X9, Canada.

[1] Corresponding author (e-mail: osherwood@gmail.com).

Can. J. Fish. Aquat. Sci. **66**: 142–152 (2009) doi:10.1139/F08-195 Published by NRC Research Press

2006). In this paper, we measure growth rates and life spans of the gorgonians *Acanella arbuscula*, *Keratoisis ornata*, *Paramuricea* spp., and *Paragorgia arborea* and antipatharian *Stauropathes arctica* collected off Newfoundland and Labrador, using the bomb-radiocarbon dating method. We also compare radial and linear growth rates in a suite of growth ring dated colonies of *P. resedaeformis* collected during a single tow in the northern Labrador Sea with growth rates from the Northeast Channel, southwest of Nova Scotia.

Oceanic uptake of bomb radiocarbon produced by atmospheric nuclear weapons testing in the late 1950s and early 1960s provides a time-varying tracer. Based on direct measurements of dissolved inorganic carbon (DIC; Nydal et al. 1998) and indirect measurements of ^{14}C in known-age proxies (Druffel 1980; Weidman and Jones 1993), the initial increase in bomb ^{14}C in surface waters of the North Atlantic occurred around 1957. This provides a unique time marker that may be used to establish or validate skeletal chronology (Kerr et al. 2005; Roark et al. 2006). If a reference bomb-^{14}C chronology is known for a particular water mass, then that itself may be used for age calibration of bomb-^{14}C data (Campana 1997; Roark et al. 2005; Sherwood et al. 2005). Potential carbon sources to deep-sea corals include particulate organic carbon (POC), sedimentary organic carbon (SOC), dissolved organic carbon (DOC), and DIC (Roark et al. 2006). Below the mixed layer of the ocean, recently exported POC is generally the only carbon source “tagged” with bomb ^{14}C; other carbon reservoirs contain typically prebomb levels of $\Delta^{14}C$ (<0‰; Druffel and Williams 1990; Druffel et al. 1992; Bauer et al. 2001). Because the organic fractions of deep-sea corals contain bomb ^{14}C, recently exported POC is thought to be their main carbon source (Griffin and Druffel 1989; Roark et al. 2005; Sherwood et al. 2005). Therefore, bomb-^{14}C measurements may be used to date deep-sea corals, assuming that there is no phase-lag or signal attenuation in the bomb-^{14}C signal in recently exported POC with depth in the water column.

Materials and methods

Since 2002, coral specimens caught opportunistically as trawl bycatch during stock assessment surveys and fisheries operations have been collected and stored by Fisheries and Oceans Canada. The sampling program and the deep-sea coral fauna of the region are described more completely in Wareham and Edinger (2007) and Edinger et al. (2007*a*). From this collection, colonies of *A. arbuscula* (Johnson, 1862), *S. arctica* (Lütken, 1871), *K. ornata* (Verrill, 1878), *P. arborea* (Linnaeus, 1758), *P. resedaeformis* (Gunnerus, 1763), and *Paramuricea grandis* (Verrill, 1884) and (or) *Paramuricea placomus* (Linnaeus, 1758) were selected. As much as possible, representative colonies of each species were selected; however, it was necessary in some cases to select larger colonies to maximize sample mass for ^{14}C analyses. Additional samples were collected using the remotely operated vehicle *ROPOS* during an expedition to the Southwest Grand Banks in July 2007. Complete sample details are provided in Table 1.

For radiocarbon analysis, approximately 0.5 cm thick cross sections were cut from the bases of colonies with an Isomet™ low-speed saw or a hand saw. The sections were ground and polished using silicon carbide films, ultrasonically cleaned in deionized water, and then photographed with a Nikon Coolpix™ 900 digital camera attached to a Nikon SZ 1000 binocular microscope. Incandescent or ultraviolet light was used to image growth rings, and resulting images were used to guide sampling. Samples were isolated in one of three ways. Isidid gorgonian corals (*A. arbuscula*, *K. ornata*) were prepared by sectioning the organic nodes from calcitic internodes and dissolving the sections in 5% HCl to remove any remaining carbonate. Individual growth rings were then teased apart with scalpel and tweezers (Sherwood et al. 2005). For the spongy skeletons of *P. arborea* and *Paramuricea* spp., a wedge was cut from each section and subsampled along its radius with a stainless-steel scalpel. Finally, *S. arctica* colonies were sectioned in half longitudinally along the skeletal axis. One-half of the longitudinal section was affixed to a glass slide with thermoplastic glue and sampled with a manual micromill. Each sample measured approximately 10 mm long × 0.5 mm wide × 1.5 mm deep, giving an approximate sample mass of 2 mg.

Samples were transferred to 5 mL polyethylene vials, topped with 5% HCl, and left for 24 h to ensure that all of the calcite dissolved. Afterwards, samples were triple-rinsed in deionized water and dried at 70 °C overnight. Decalcification was not done for *S. arctica* as it does not contain any carbonate. Samples were combusted in individual quartz tubes and reduced to graphite in the presence of iron catalyst. Radiocarbon measurements were performed on graphite targets at the Centre for Accelerator Mass Spectrometry, Lawrence Livermore National Laboratory. Results include a background and $\delta^{13}C$ correction and are reported as $\Delta^{14}C \pm 1\sigma$ error according to Stuiver and Polach (1977). Measurement of $\delta^{13}C$ was performed at Memorial University on a Finnigan™ MAT252 isotope ratio mass spectrometer following standard procedures, and values ranged from –20‰ to –17‰.

Calibration of bomb-^{14}C data

Coral $\Delta^{14}C$ data were calibrated using bomb-^{14}C reference chronology (Fig. 1*a*), based on three independently dated colonies of *P. resedaeformis* collected near the eastern entrance to Hudson Strait (samples 1525-1, 1525-3, 1525-10; 60°30′N, 61°24′W) and one colony of *K. ornata* from the southwest Grand Banks (sample 1343; 44°7′N, 52°56′W; Sherwood et al. 2008). The *P. resedaeformis* colonies were dated by counting the annual growth rings viewed in cross sections. Previous work has proven that growth rings in this species form with annual periodicity in both Northeast Pacific (Andrews et al. 2002) and Northwest Atlantic environments (Sherwood et al. 2005). Each colony was dated by three amateur counters, as described in Sherwood et al. (2005). Calendar ages were averaged over the three trials, and resulting mean ages were paired with the individual rings isolated for ^{14}C analysis. The colony of *K. ornata* was dated by conventional ^{210}Pb dating of a calcite internode sectioned from the base of the colony. The ^{210}Pb data were used to calculate the growth rate and the age of the section from the margin to the core by fitting the data with a decay curve with the ^{210}Pb decay constant ($0.03067\cdot\text{year}^{-1}$). The adjacent gorgonin node, sampled for

Table 1. Collection details, ages, and growth rates (GR) of antipatharian and gorgonian (Order Alcyonacea) corals collected off Newfoundland and Labrador.

Order/Family/Species	Sample identification	Latitude (N)	Longitude (W)	Depth (m)	Year of collection	Dating method	Age (years)	Radial GR (μm·year^{-1})	Axial GR (cm·year^{-1})
Antipatharia									
Schizopathidae									
Stauropathes arctica	465	44°34.02′	53°46.02′	876	2005	Bomb ^{14}C	55±8	66±11	1.36±0.20
Stauropathes arctica	2440	44°57.45′	55°1.19′	812	2007	Bomb ^{14}C	82±31	33±11	1.22±0.46
Alcyonacea									
Isididae									
Acanella arbuscula	1591	65°7.86′	58°27.12′	526	2006	Bomb ^{14}C[c]	<100	>20	>0.30
						Growth rings[d]	30	70	1.00
Keratoisis ornata	2452	44°49.96′	54°28.13′	601	2007	Bomb ^{14}C	94±7	74±6	0.93±0.08
Keratoisis ornata	1449[a]	61°36.00′	60°22.98′	1193	2007	^{14}C	200±30	75±11	n/a
Keratoisis ornata	1343[b]	44°7.98′	52°55.98′	713	2006	^{210}Pb	138±23	53±9	n/a
Plexauridae									
Paramuricea spp.	1348	44°13.02′	53°0.00′	814	2006	Bomb ^{14}C	103±14	92±18	0.58±0.08
Paramuricea spp.	1886	55°13.14′	55°10.98′	850	2006	Bomb ^{14}C	71±6	205±20	0.56±0.05
Paragorgiidae									
Paragorgia arborea	1523	60°29.88′	61°23.70′	414	2006	Bomb ^{14}C	80±11	830±120	1.62±0.22
Primnoidae									
Primnoa resedaeformis	1525-1[b]	60°29.88′	61°23.70′	414	2006	Growth rings[e]	50±3	n/a	n/a
Primnoa resedaeformis	1525-3[b]	60°29.88′	61°23.70′	414	2006	Growth rings[e]	100±9	90±8	1.00±0.09
Primnoa resedaeformis	1525-4	60°29.88′	61°23.70′	414	2006	Growth rings[f]	72±4	146±8	n/a
Primnoa resedaeformis	1525-5	60°29.88′	61°23.70′	414	2006	Growth rings[f]	31±4	165±21	1.71±0.22
Primnoa resedaeformis	1525-6	60°29.88′	61°23.70′	414	2006	Growth rings[f]	23±4	215±37	2.61±0.45
Primnoa resedaeformis	1525-7	60°29.88′	61°23.70′	414	2006	Growth rings[f]	24±4	188±31	2.50±0.42
Primnoa resedaeformis	1525-8	60°29.88′	61°23.70′	414	2006	Growth rings[f]	24±4	167±28	2.29±0.38
Primnoa resedaeformis	1525-10[b]	60°29.88′	61°23.70′	414	2006	Growth rings[e]	44±3	125±9	1.86±0.13
Primnoa resedaeformis	1526-1	60°10.56′	61°47.40′	257	2006	Growth rings[f]	50±4	130±10	n/a
Primnoa resedaeformis	1526-2	60°10.56′	61°47.40′	257	2006	Growth rings[f]	57±4	105±7	n/a
Primnoa resedaeformis	1534	61°29.28′	61°49.14′	608	2006	Growth rings[f]	52±4	83±6	n/a
Primnoa resedaeformis	1536-1	61°12.12′	61°22.68′	585	2006	Growth rings[f]	18±4	194±43	1.94±0.43
Primnoa resedaeformis	1536-2	61°12.12′	61°22.68′	585	2006	Growth rings[f]	20±4	170±34	1.80±0.36
Primnoa resedaeformis	1539	60°19.38′	62°8.94′	285	2006	Growth rings[f]	18±4	181±40	n/a
Primnoa resedaeformis	1567	62°9.66′	61°32.22′	456	2006	Growth rings[f]	62±4	121±8	n/a
Primnoa resedaeformis	2370-1	61°21.00′	60°40.98′	640	2006	Growth rings[f]	42±4	194±18	1.90±0.18

Note: Additional samples not dated by the bomb-^{14}C method are included for comparison. n/a, not available.

[a] Subfossil specimen (Sherwood et al., unpublished data).

[b] Specimens included in reference chronology (Sherwood et al., unpublished data).

[c] Too few bomb-^{14}C data points to constrain absolute age and growth rate.

[d] Assuming growth rings are formed annually.

[e] Growth ring counting followed procedure in Sherwood et al. (2005) using three counters. Error reported as ±1 SD.

[f] Growth rings counted by one counter. Age error estimated as ±4 years following Sherwood et al. (2005).

Fig. 1. (*a*) Bomb-^{14}C reference chronology for the offshore branch of the Labrador Current off Newfoundland and Labrador, derived from growth ring dated colonies of *Primnoa resedaeformis* from the Hudson Strait (□) and a ^{210}Pb-dated colony of *Keratoisis ornata* from the Grand Banks (■; Sherwood et al. 2008). Data have been fitted with a Loess curve, bounded by the 95% prediction intervals. (*b*) Example calibration of a hypothetical data set with fixed values of distance (±1/2 sample width) and Δ^{14}C (±1 σ error). Distances are converted to calendar years depending on a chosen growth rate. At the minimum growth rate (△), the error bar of the middle data point almost loses contact with prediction band of the reference chronology. At the maximum growth rate (▽), the oldest data point almost loses contact with the reference chronology. At the average of the minimum and maximum growth rates (■), all of the data are enclosed within the prediction bands.

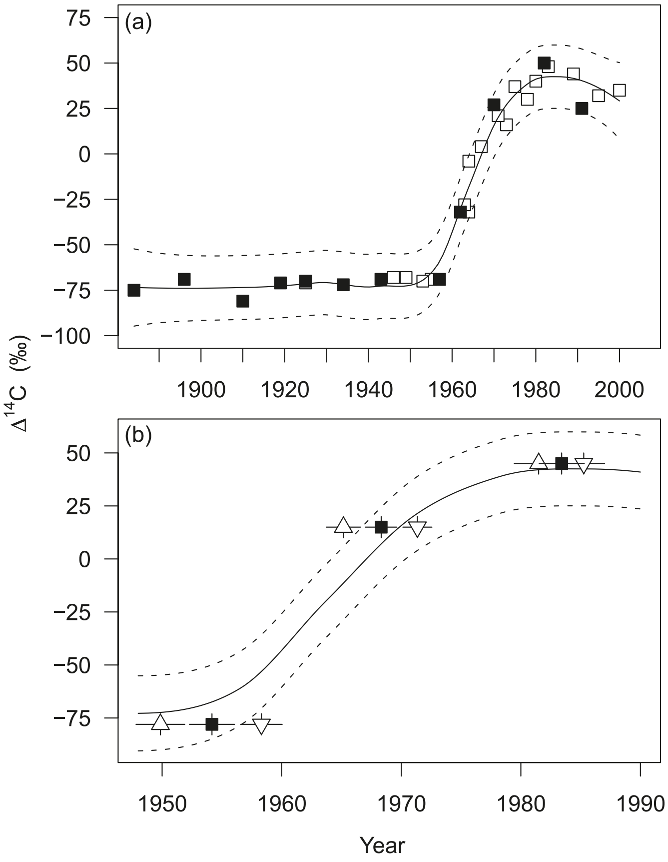

^{14}C, was located <5 mm away from the internode section and was assumed to have the same age, within the dating error. From this age, growth rate and sample ages were recalculated across the radius of the node. Bomb-^{14}C chronologies from the two sites were identical, so the data were merged to produce a single reference chronology representing surface waters of the offshore branch of the Labrador Current off Newfoundland and Labrador. During the prebomb era (pre-1957), values of Δ^{14}C were stable at ~−70‰. Beginning in 1957, Δ^{14}C increased rapidly, paralleling the rise in atmospheric Δ^{14}C (Levin and Kromer 2004). Values of Δ^{14}C peaked at ~+50‰ around 1985, then decreased to ~+30‰ by the year 2000. Alternative bomb-^{14}C chronologies have been developed from otoliths of known-age fish sampled from the southwest Grand Banks (NAFO Division 3Ps) and the northern and western margins of the Labrador Sea (NAFO Divisions 0B, 1ABCDEF, 2GJ; Campana et al. 2008). In all of the chronologies, bomb ^{14}C began to increase around the year 1957; however, the signals differ in timing and magnitude of the bomb-^{14}C peak because of water mass mixing at the various sites (Sherwood et al. 2008). Therefore, our coral-based record was chosen as the reference chronology because it better reflects the slope-water region of Newfoundland and Labrador.

For each coral section to be dated, between two and four samples were isolated for Δ^{14}C, representing some combination of prebomb, bomb-increase, and postbomb data points. Calibration of Δ^{14}C data to constrain growth rates was performed using an iterative graphical procedure (Fig. 1*b*). For each coral, sample radial distances (±1/2 sample widths) were converted to calendar years (± year errors) by dividing by an estimated growth rate. Data were then plotted as Δ^{14}C vs. calendar year and compared with the reference chronology. This procedure was repeated sequentially with a range of growth rates in increments of 1 μm·year^{-1}. Minimum and maximum growth rates were constrained as the limits in which all of the data points, including error bars, remained in contact with the 95% prediction intervals enveloping the reference chronology. The average (±1/2 the range) of the minimum and maximum growth rates is reported throughout this paper. Sample age was calculated by applying the growth rate over the radius of the coral.

Enumeration of growth rings

With the exception of *P. arborea*, which does not exhibit growth rings, and *P. resedaeformis*, which was already known to secrete annual growth rings (Andrews et al. 2002; Sherwood et al. 2005), all of the remaining species exhibited concentric growth rings of unknown periodicity. To estimate their periodicity, ring widths were compared with radial growth rates determined using bomb-^{14}C dating. Ring widths were measured by counting the number of rings across the same radius from which samples for ^{14}C were isolated and dividing that number by the distance. In some cases, enumeration of growth rings was limited to part of the radius, because of inconsistent clarity. If the average width of growth rings matched the bomb-^{14}C-derived growth rate, within error, this was interpreted as evidence for annual periodicity of growth rings.

Results

Two colonies of *S. arctica* were examined for Δ^{14}C. This species displayed clearly visible growth rings when viewed as thick sections illuminated with ultraviolet light, or as thin sections viewed with either ultraviolet or transmitted light (Fig. 2*a*). Rings consisted of alternating light brown (luminescent) and dark brown (nonluminescent) couplets. Colony 465 was collected from the Labrador Slope at a depth of 876 m (Table 1). There were 53 growth rings, averaging 60 μm in width. Radiocarbon data constrained the radial growth rate to 66 ± 11 μm·year^{-1} and the age of the section to 55 ± 8 years (Fig. 2*b*). Another colony (2440) was collected from the southwest Grand Banks at a depth of 812 m (Table 1). In this colony, there were 58 growth

Fig. 2. (*a*) Basal thin section through the axial skeleton of *S. arctica* No. 465, illuminated with ultraviolet light. Growth rings are delineated by white hatches. Numbers 1–4 indicate the locations of samples milled for ^{14}C analysis. (*b*) The reference bomb-^{14}C chronology overlain with data for colony 465 (■) and colony 2440 (□). Sample distances are indicated along the upper horizontal axes. For colony 465, bomb-^{14}C data constrained the radial growth rate to between 55 and 76 μm·year^{-1}; data are plotted at the average of 66 μm·year^{-1}. For colony 2440, bomb-^{14}C data constrained the radial growth rate to between 22 and 44 μm·year^{-1}; data are plotted at the average of 33 μm·year^{-1}. Horizontal error bars indicate the width of individual samples converted to calendar years at indicated average growth rate. Vertical error bars are smaller than symbols.

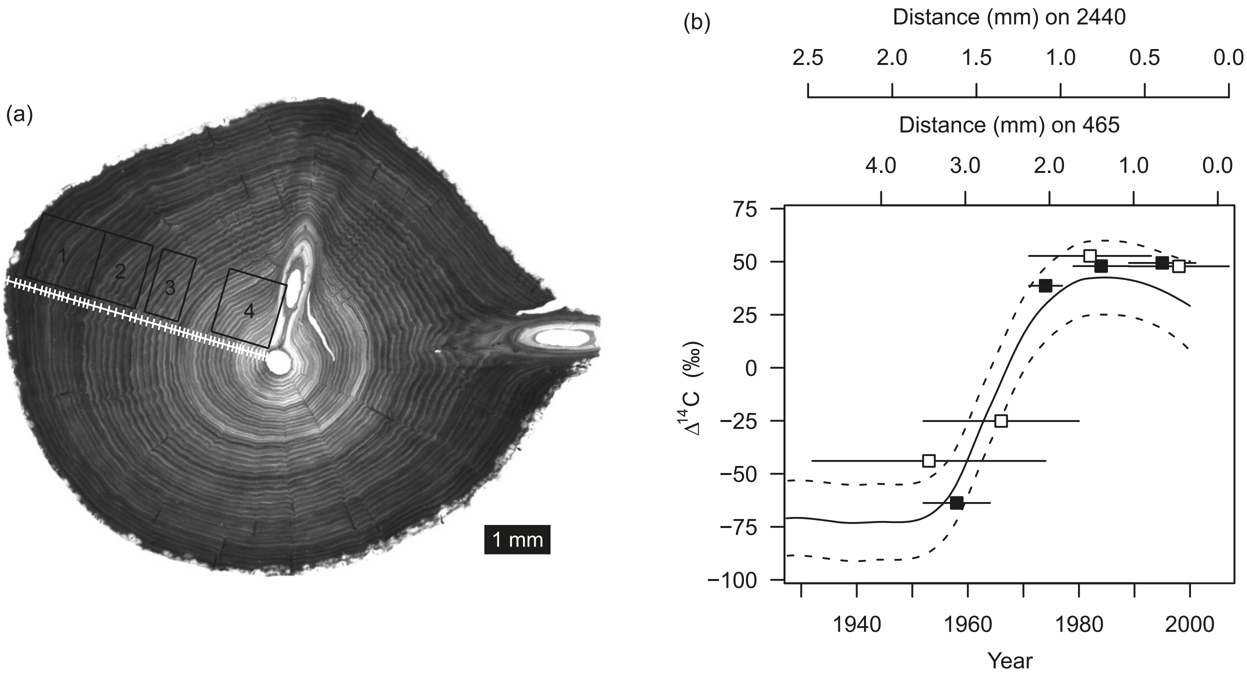

rings, averaging 46 μm in width. Radiocarbon data constrained the radial growth rate to 33 ± 11 μm·year^{-1} and the age to 82 ± 31 years. This colony had a thinner skeletal axis, accounting for the larger errors in growth rate and age, as milled samples integrated over a wider range of growth rings. In both colonies, similarity between bomb-^{14}C-derived growth rates and rings widths provides strong evidence that the growth rings are formed annually.

A colony of *K. ornata* (No. 2452) was collected from the southern Grand Banks at a 601 m depth (Table 1). In cross section, organic nodes exhibited alternating light and dark concentric growth rings (Fig. 3*a*). Rings were easier to visualize in thick section under incident light than in thin section under transmitted light. Clarity of the rings varied from poor towards the middle of the section to good in the middle and outer regions of the section, where they averaged 80 μm in width. Four individual growth rings were isolated and analysed for Δ^{14}C, which constrained the radial growth rate to 74 ± 6 μm·year^{-1} and the age to 94 ± 7 years (Fig. 3*b*). Close correspondence between the bomb-^{14}C-derived growth rate and the width of the growth rings is strong evidence that the growth rings in this species are formed annually.

A colony of *A. arbuscula* (No. 1591) was collected from the Davis Strait area at a depth of 526 m (Table 1). Skeletons of *A. arbuscula* are like those of *K. ornata*, but much smaller. Colony diameters rarely exceed 4 mm, making them difficult to sample. In cross section, the organic nodes exhibited concentric growth rings, similar to those observed in *K. ornata*, averaging 70 μm in width (Fig. 4*a*). Outer, middle, and inner regions of the node were isolated for Δ^{14}C, but the inner sample was too small for analysis. Outer and middle samples produced Δ^{14}C values typical of the postbomb era. Because of this, only a minimum radial growth rate of 20 μm·year^{-1} (age < 100 years) could be determined. Based on the finding that growth rings in *K. ornata* appear to form annually, this was assumed in *A. arbuscula* as well. Using a rate of 70 μm·year^{-1} (i.e., the width of the growth rings), Δ^{14}C values plotted well within the 95% prediction intervals of the reference chronology (Fig. 4*b*). The corresponding age was 30 years. This was taken as tentative support for annual timing of growth rings in *A. arbuscula*, but more data are needed for verification.

Two colonies of *Paramuricea* spp. were examined (Table 1). Colony 1886 was collected from the central Labrador Slope at a depth of 850 m. A basal cross section exhibited seven diffuse growth rings averaging 2 mm in width (Fig. 5*a*). Radiocarbon data constrained the radial growth rate to 205 ± 20 μm·year^{-1} and the age to 71 ± 6 years. Given this age, the seven visible growth rings appear to have formed approximately once every 10 years. Another colony (No. 1348) was collected from the southwest Grand Banks at a depth of 814 m. In cross section, continuous growth rings were not observed. Δ^{14}C data constrained the radial growth rate to 92 ± 18 μm·year^{-1} and the age to 103 ± 14 years.

A large, 130 cm high colony of *P. arborea* (No. 1523) was collected from the Hudson Strait area at a depth of 414 m (Table 1). *Paragorgia arborea* has a porous texture, with the pores aligned somewhat concentrically (Fig. 6*a*);

Fig. 3. (*a*) Thick section through a basal node of *K. ornata* No. 2452. Growth rings, where visible, are delineated by white hatches. Numbered arrows point to individual rings isolated for ^{14}C analysis. (*b*) Reference bomb-^{14}C chronology overlain with data for colony 2452. Bomb-^{14}C data constrained the radial growth rate to between 68 and 79 μm·year^{-1}; data are plotted at the average of 74 μm·year^{-1}.

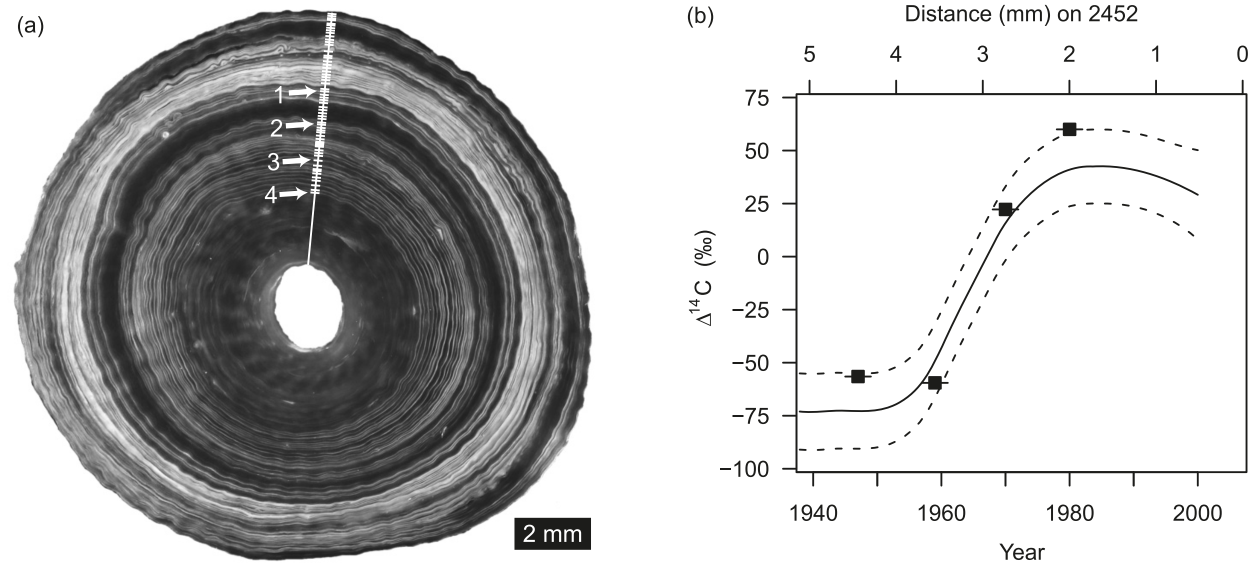

Fig. 4. (*a*) Close-up of a thick section through a basal node of *A. arbuscula* No. 2452. Numbers indicate samples for ^{14}C analysis. Growth rings are delineated by solid circles. (*b*) Reference bomb-^{14}C chronology overlain with data for colony 1591. Because only two samples were measured, Δ^{14}C did not constrain an absolute growth rate, but rather only a minimum of >20 μm·year^{-1}. Data were therefore replotted at a growth rate of 70 μm·year^{-1}, as indicated by the width of the growth rings, assuming that they form annually.

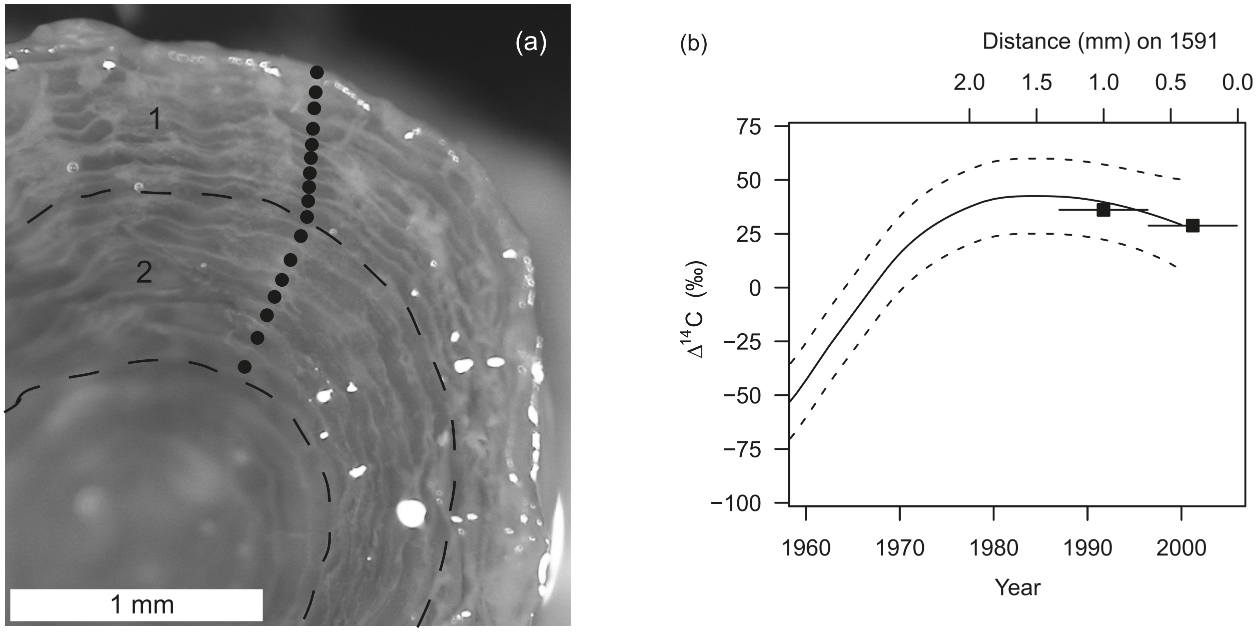

however, continuous growth rings could not be visualized, as previously reported for this species (Mortensen and Buhl-Mortensen 2005). Three samples were isolated for Δ^{14}C; calibration of the middle sample to the period of bomb-^{14}C increase constrained the radial growth rate to 830 ± 120 μm·year^{-1} (Fig. 6*b*). At this growth rate, however, the oldest sample plotted slightly outside the 95% prediction intervals of the reference curve during the prebomb period. We suspect that this sample may have been contaminated with younger carbon. Alternatively, the radial growth rate may have been significantly higher during the first half of the life of the colony. Additional data points would be needed to resolve this question.

Plots of radius vs. age and axial height vs. age for all of the colonies above, with additional data for conventional ^{14}C- and ^{210}Pb-dated colonies of *K. ornata* and growth ring dated colonies of *P. resedaeformis* are shown (Fig. 7). Radial growth rates delimit the coral species into three groups (Fig. 7*a*); *S. arctica*, *K. ornata*, and *A. arbuscula* had the

Fig. 5. (*a*) Basal thick section of *Paramuricea* spp. colony 1886. Numbered segments indicate the locations of samples isolated for $\Delta^{14}C$ analysis. Solid circles indicate concentric growth rings forming with an apparent periodicity of ~10 years. (*b*) Reference bomb-^{14}C chronology overlain with data for colony 1886 (open squares) and colony 1348 (solid squares). For colony 1886, bomb-^{14}C data constrained the radial growth rate to between 185 and 224 μm·year^{-1}; data are plotted at the average of 205 μm·year^{-1}. For colony 1348, bomb-^{14}C data constrained the radial growth rate to between 74 and 110 μm·year^{-1}; data are plotted at the average of 92 μm·year^{-1}.

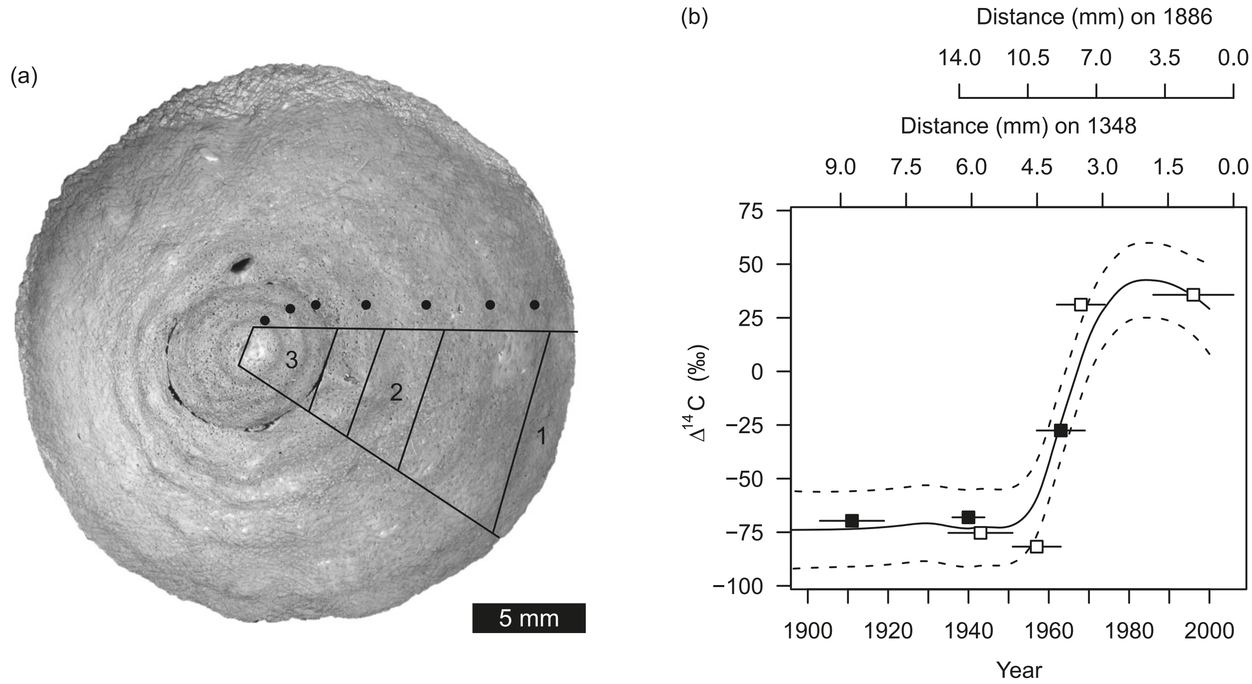

Fig. 6. (*a*) Basal thick section of *Paragorgia arborea* No. 1523. Numbered segments indicate the locations of samples isolated for $\Delta^{14}C$ analysis. Note skeletal porosity and lack of visible growth rings. (*b*) Reference bomb-^{14}C chronology overlain with data for colony 1523. Bomb-^{14}C data constrained the radial growth rate to between 710 and 950 μm·year^{-1}; data are plotted at the average of 830 μm·year^{-1}. The oldest data point plots slightly outside the 95% prediction intervals of the reference chronology, perhaps indicating reworking of the skeletal matrix and (or) nonlinear radial growth.

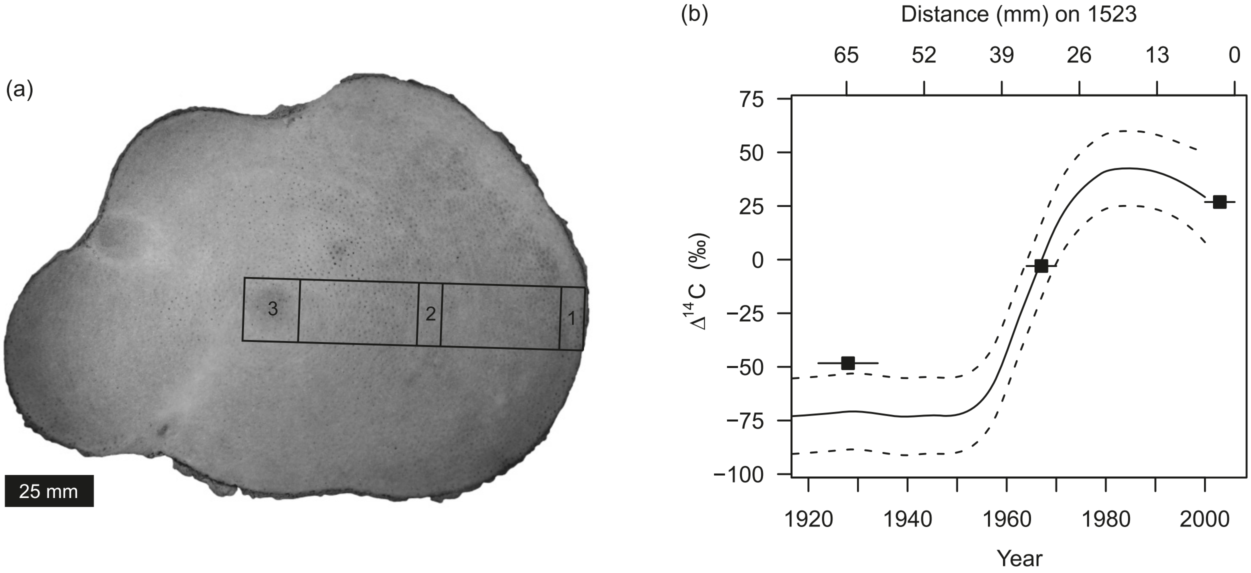

lowest growth rates, ranging from 33 ± 11 to 75 ± 11 μm·year^{-1}. *Paramuricea* spp. and *P. resedaeformis* had faster radial growth rates, ranging from 83 ± 6 to 215 ± 37 μm·year^{-1}. Finally, *P. arborea* thickens much faster than any of the other species, at 830 ± 120 μm·year^{-1}. Axial growth rates ranged from 0.56 ± 0.05 cm·year^{-1} for *Paramuricea* spp. to 2.61 ± 0.45 cm·year^{-1} for *P. resedaeformis* (Fig. 7*b*).

Plots of radius vs. age and axial height vs. age for two different populations of *P. resedaeformis* collected from the Hudson Strait (Table 1) and the Northeast Channel, southwest of Nova Scotia (Mortensen and Buhl-Mortensen 2005)

Fig. 7. (*a*) Skeletal radius vs. age for deep-sea antipatharians and gorgonians off Newfoundland and Labrador: *Stauropathes arctica*, ■; *Keratosis ornata*, ▲; *Acanella arbuscula*, ▼; *Paramuricea* spp., □; *Paragorgia arborea*, △; *Primnoa resedaeformis*, ▽. Reference lines indicate growth rates of 50 and 150 μm·year^{-1}. (*b*) Axial height vs. age for the same colonies (where available). Reference lines indicate axial growth rates of 0.5 and 2 mm·year^{-1}.

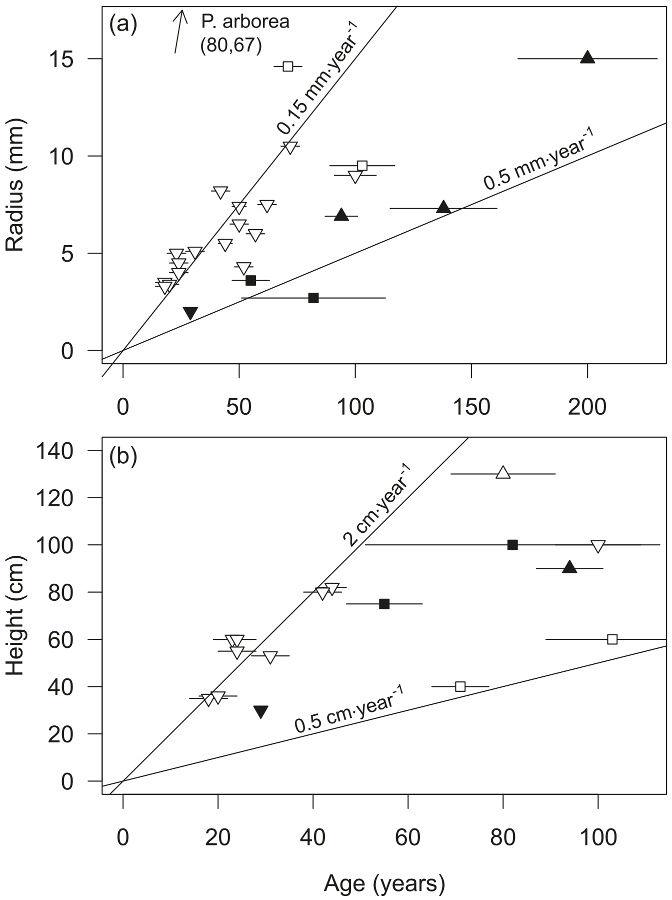

Fig. 8. Comparison of (*a*) radial and (*b*) axial growth rates in colonies of *Primnoa resedaeformis* collected from the Hudson Strait (this study; ■) and the Northeast Channel (Mortensen and Buhl-Mortensen 2005; □). In both cases, logarithmic fits were superior to linear fits, as indicated by r^2 values. Radial growth rates were significantly higher at the Northeast Channel than at the Hudson Strait, but axial growth rates were not.

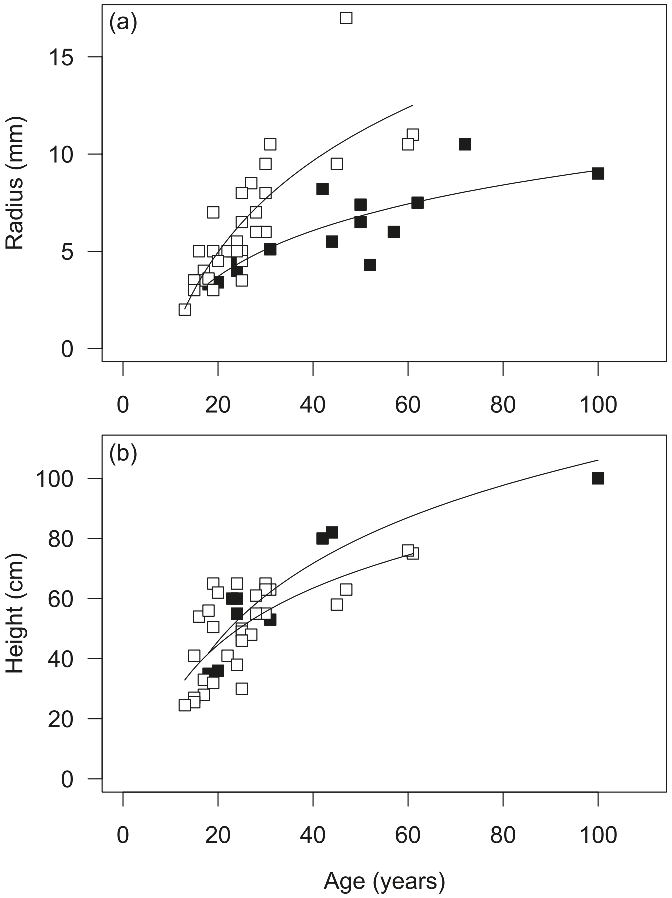

are shown (Fig. 8). The Northeast Channel population had a significantly higher radial growth rate (230 ± 60 μm·year^{-1}) than the Hudson Strait population (151 ± 39 μm·year^{-1}; *t* test, $p < 0.001$; Fig. 8*a*), but there was no significant difference in axial growth rates between the two populations (Fig. 8*b*).

Discussion

The presence of bomb radiocarbon in all of the species examined here adds further support to the theory that recently fixed and exported POM is the primary source of carbon to the organic endoskeletons of deep-sea gorgonians and antipatharians. Bomb-^{14}C dating relies on the assumption that there is no phase-lag or signal attenuation with depth. Relative to surface water bomb-^{14}C chronologies, deep-water chronologies derived from the skeletal carbonate of deep-sea corals (Sherwood et al. 2008) and from otoliths of deep-dwelling fish (Campana et al. 2008) are both lagged and attenuated. Maximum levels of bomb ^{14}C in our unknown-age corals did not appear attenuated with respect to the reference chronology, perhaps with the exception of *A. arbuscula* and *P. arborea*, for which more data were needed to resolve the bomb peak. Therefore, we conclude that it is unlikely that bomb-^{14}C data from unknown-age colonies were phase-lagged. Consequently, the bomb-^{14}C dating method provided robust estimates of growth rates and ages. Errors averaged 20%. It is doubtful that this error could be much improved, even with tighter sampling across the skeletons, because of the variability in radial growth rates evident in the asymmetric shape of skeletal cross sections. For example, the difference between maximum and minimum radial growth rates ranged from 14% for *K. ornata* (No. 1343) to 52% for *P. arborea* (No. 1523).

Bomb-^{14}C dating may be compromised where younger carbon is exchanged with older parts of the skeleton, for example, by the actions of boring organisms (Boerboom et al. 1998) or by secondary ingrowth around the central core of the skeletal axis (Lewis et al. 1992; Tracey et al. 2007). This may have been the case with the innermost sample of *P. arborea* (No. 1523). High skeletal porosity in this species may facilitate the reworking of the skeletal matrix (Andrews et al. 2005). *Paramuricea* spp. also forms a spongy axis without clearly delineated growth rings, but there was no indication of reworking. The remaining species have consolidated axes that are much more resistant to reworking.

Concentric growth rings in gorgonian and antipatharian corals are often assumed to form annually, but this is rarely validated for particular species and locations using independent dating methods. In addition to *P. resedaeformis* growing off eastern Canada (Sherwood et al. 2005), bomb radiocarbon data show that three additional species (*A. arbuscula*, *K. ornata*, and *S. arctica*) also secrete annual growth rings in their axial skeletons. *Acanella arbuscula* and *K. ornata* are in the same family (Isididae), so it is not surprising that they exhibit similar growth ring morphology and periodicity. In both species, growth rings were visualized in the organic nodes of the skeletal axes and consisted of alternating light brown and dark brown couplets. Color variation may have to do with differences in protein tanning, as suggested for shallow-water gorgonians (Szmant-Froelich 1974), but this remains untested. Unfortunately, inconsistent clarity of growth rings may limit their use in dating colonies of *A. arbuscula* and *K. ornata* without independent validation. Growth rings in the calcite internodes, as opposed to the organic nodes studied here, of Isidid corals have also been described, but poor clarity and unclear periodicity make them unreliable as an indicator of colony age (Thresher et al. 2004; Andrews et al. 2005; Tracey et al. 2007). Roark et al. (2005), however, were successful in counting growth rings in the calcitic internodes of Alaskan Isidids. Growth rings in *S. arctica* were of more consistent clarity. Use of ultraviolet light improved ring discrimination tremendously because the growth rings consist of alternating layers of chitin (fluorescent) and nonfibrillar protein (nonfluorescent; Kim et al. 1992). Clarity of growth rings in this species suggests that this could be used to date large numbers of colonies relatively quickly and inexpensively. In contrast, growth rings in *Paramuricea* spp. did not form annually and should not be relied upon to date colonies (cf. Mistri and Ceccherelli 1994), whereas growth rings in *P. arborea* could not be visualized at all.

Growth rates of Newfoundland and Labrador corals match very closely with growth rates in related taxa from different regions of the world. The antipatharian *S. arctica* had the lowest radial growth rate of 33 ± 11 to 66 ± 11 μm·year^{-1}. Antipatharians, in general, are some of the slowest-growing deep-sea corals, with radial growth rates of ~15 μm·year^{-1} for *Leiopathes glaberrima* collected off Florida, USA (Williams et al. 2006) and ≤10 μm·year^{-1} (age > 2000 years) for *L. glaberrima* collected off Hawaii (Roark et al. 2006). Isidid corals (*A. arbuscula*, *K. ornata*) had similarly low radial growth rates of 53 ± 9 to 75 ± 11 μm·year^{-1}. Similar values were reported for bamboo corals collected off California (50–110 μm·year^{-1}; Andrews et al. 2005), the Gulf of Alaska (50–60 μm·year^{-1}; Roark et al. 2005), Tasmania (~100 μm·year^{-1}; Thresher et al. 2007), and New Zealand (130–290 μm·year^{-1}; Tracey et al. 2007). Radial growth rates for *P. arborea* have not been reported previously using radiometric techniques; however, axial growth rates have been estimated at 0.8–4 cm·year^{-1} for *P. arborea* specimens from New Zealand (Tracey et al. 2003) and Norway (Mortensen and Buhl-Mortensen 2005), similar to the 1.62 ± 0.22 cm·year^{-1} in our Hudson Strait specimen. To our knowledge, these are the first estimates of radial (92 ± 18 μm·year^{-1} to 205 ± 20 μm·year^{-1}) and axial (0.56 ± 0.05 μm·year^{-1} to 0.58 ± 0.08 cm·year^{-1}) growth rates for deep-sea *Paramuricea* spp.; shallow-water congeners grow at slightly faster axial growth rates (1.8 cm·year^{-1}; Coma et al. 1998).

Similarities and differences in growth rates between species may reflect, in part, mechanical requirements of skeletal axes. For example, *P. resedaeformis* and *P. arborea* inhabit relatively shallow, faster-current environments. *Primnoa resedaeformis* forms stiff, consolidated axes. The weaker, unconsolidated axes of *P. arborea* require a greater degree of axial thickening to withstand the same current velocities. By contrast, *S. arctica*, Isidids, and *Paramuricea* spp. all mostly inhabit relatively deeper, slower-current environments. *Stauropathes arctia* and Isidids form stiff axes requiring less axial thickening than the weaker, spongy axes of *Paramuricea* spp. in a similar a current regime.

Differences in radial growth rates between populations of the same species may reflect adaptations to local current regimes. For example, there was a significant difference in radial growth rates among Northeast Channel and Hudson Strait populations of *P. resedaeformis*. Faster radial growth rates in the Northeast Channel population may be a response to the strong tidal currents, which average 100 cm·s^{-1} in this submarine canyon (current meter data retrieved from area SS29 in the Ocean Data Inventory, available online at http://www.mar.dfo-mpo.gc.ca/science/ocean/database/data_query.html). The Hudson Strait population was sampled near the Hatton Basin, a large, bowl-shaped bathymetric depression to the east of Hudson Strait, where current velocities average only 40 cm·s^{-1}. Lack of difference in axial growth rates between these two populations suggests that axial growth rates may be less sensitive to the influence of current velocities than radial growth rates.

Overall, our results show that deep-sea corals off Newfoundland and Labrador are slow-growing and long-lived. All of the specimens reported on here were collected from heavily fished areas, with the exception of the Hudson Strait (Edinger et al. 2007*b*). The largest and oldest colonies are likely to have already been removed from the population, thereby biasing age distributions toward smaller and younger colonies (cf. Anderson and Clarke 2003). This may explain why exceptionally large and old colonies (>100 years) collected off eastern Canada are usually subfossil in age. Little is known about the frequency of recruitment events in deep-sea gorgonians and antipatharians; however, knowledge of shallow-water taxa (Grigg 1977; Farrant 1987; Lasker et al. 1998) and preliminary evidence from deep-sea species (Mills and Mullineaux 2005) suggest that it may be infrequent. The combination of great longevity, slow growth rates, and infrequent recruitment implies that populations of deep-sea corals damaged by fishing gear will take centuries to recover. Conservation measures to protect deep-sea corals off Newfoundland and Labrador should be designed and implemented immediately.

Acknowledgements

We thank the fisheries observers, the officers and crews of the CCGS *Hudson*, *Teleost*, and *Wilfred Templeman*, and

ROPOS technicians for their help in acquiring samples. Kent Gilkinson and Vonda Wareham provided logistical support. We also thank Pål Mortensen for sharing growth rate data on Northeast Channel samples and Tom Guilderson and Bruce Buchholz for AMS analyses. Comments by Allen H. Andrews and an anonymous reviewer led to significant improvement of the manuscript. This work was funded by the Fisheries and Oceans Canada International Governance of High Seas Fisheries (IGP) program, a Natural Sciences and Engineering Research Council of Canada (NSERC) Discovery grant to E.E., and an NSERC postdoctoral fellowship to O.A.S.

References

Anderson, O.F., and Clarke, M.R. 2003. Analysis of bycatch in the fishery for orange roughy (*Hoplostethus atlanticus*) on the South Tasman Rise. Mar. Freshw. Res. **54**: 643–652. doi:10.1071/MF02163.

Andrews, A.H., Cordes, E.E., Mahoney, M.M., Munk, K., Coale, K.H., Cailliet, G.M., and Heifetz, J. 2002. Age, growth and radiometric age validation of a deep-sea, habitat-forming gorgonian (*Primnoa resedaeformis*) from the Gulf of Alaska. Hydrobiologia, **471**: 101–110. doi:10.1023/A:1016501320206.

Andrews, A.H., Cailliet, G.M., Kerr, L.A., Coale, K.H., Lundstrom, C., and DeVogelaere, A.P. 2005. Investigations of age and growth for three deep-sea corals from the Davidson Seamount off central California. *In* Cold-water corals and ecosystems. *Edited by* A. Friewald and J.M. Roberts. Springer-Verlag, Berlin, Germany. pp. 1021–1038.

Bauer, J.E., Druffel, E.R.M., Wolgast, D.M., and Griffin, S. 2001. Cycling of dissolved and particulate organic radiocarbon in the Northwest Atlantic continental margin. Global Biogeochem. Cycles, **15**(3): 615–636. doi:10.1029/2000GB001314.

Boerboom, C.M., Smith, J.E., and Risk, M.J. 1998. Bioerosion and micritisation in the deep-sea coral *Desmophyllum cristagalli*. Hist. Biol. **13**: 53–60.

Campana, S.E. 1997. Use of radiocarbon from nuclear fallout as a dated marker in the otoliths of haddock *Melanogrammus aeglefinus*. Mar. Ecol. Prog. Ser. **150**: 49–56. doi:10.3354/meps150049.

Campana, S.E., Casselman, J.M., and Jones, C.M. 2008. Bomb radiocarbon chronologies in the Arctic, with implications for the age validation of lake trout (*Salvelinus namaycush*) and other Arctic species. Can. J. Fish. Aquat. Sci. **65**: 733–743. doi:10.1139/F08-012.

Coma, R., Ribes, M., Zabala, M., and Gili, J.-M. 1998. Growth in a modular colonial marine invertebrate. Estuar. Coast. Shelf Sci. **47**: 459–470. doi:10.1006/ecss.1998.0375.

Druffel, E.R.M. 1980. Radiocarbon in annual coral rings of Belize and Florida. Radiocarbon, **22**: 363–371.

Druffel, E.R.M., and Williams, P.M. 1990. Identification of a deep marine source of particulate organic carbon using bomb ^{14}C. Nature (London), **347**: 172–174. doi:10.1038/347172a0.

Druffel, E.R.M., Williams, P.M., Bauer, J.E., and Ertel, J.R. 1992. Cycling of dissolved and particulate organic matter in the open ocean. J. Geophys. Res. C Oceans, **97**: 15639–15659. doi:10.1029/92JC01511.

Edinger, E.N., Wareham, V.E., and Haedrich, R.L. 2007*a*. Patterns of groundfish diversity and abundance in relation to deep-sea coral distributions in Newfoundland and Labrador waters. *In* Conservation and adaptive management of seamount and deep-sea coral ecosystems. *Edited by* R.Y. George and S.D. Cairns. Bull. Mar. Sci. **81**(Suppl. 1): 101–122.

Edinger, E.N., Baker, K.D., Devillers, R.D., and Wareham, V.E. 2007*b*. Cold-water corals in waters off Newfoundland and Labrador: distributions and fisheries impacts. World Wildlife Fund Canada, Toronto, Ontario.

Farrant, P.A. 1987. Population dynamics of the temperate Australian soft coral *Capnella gaboensis*. Mar. Biol. (Berl.), **96**: 401–407. doi:10.1007/BF00412524.

Freiwald, A., and Roberts, J.M. 2005. Cold-water corals and ecosystems. Springer-Verlag, Berlin, Germany.

Gass, S.E., and Willison, J.H.M. 2005. An assessment of the distribution of deep-sea corals in Atlantic Canada by using both scientific and local forms of knowledge. *In* Cold-water corals and ecosystems. *Edited by* A. Friewald and J.M. Roberts. Springer-Verlag, Berlin, Germany. pp. 223–245.

Griffin, S., and Druffel, E.R.M. 1989. Sources of carbon to deep-sea corals. Radiocarbon, **55**: 533–542.

Grigg, R.W. 1977. Population dynamics of two gorgonian corals. Ecology, **58**: 278–290. doi:10.2307/1935603.

Haedrich, R.L., Merrett, N.R., and O'Dea, N.R. 2001. Can ecological knowledge catch up with deep-water fishing? A North Atlantic perspective. Fish. Res. **35**: 1–10.

Hall-Spencer, J., Allain, V., and Fosså, J.H. 2002. Trawling damage to Northeast Atlantic ancient coral reefs. Proc. R. Soc. Lond. B Biol. Sci. **269**: 507–511. doi:10.1098/rspb.2001.1910.

Kerr, L.A., Andrews, A.H., Munk, K., Cailliet, G.M., Coale, K.H., Brown, T.A., and Frantz, B.R. 2005. Age validation of quillback rockfish (*Sebastes maliger*) using bomb radiocarbon. Fish. Bull. (Washington, D.C.), **103**: 97–107.

Kim, K., Goldberg, W.M., and Taylor, G.T. 1992. Architectural and mechanical properties of the Black Coral skeleton (Coelenterata: Antipatharia): a comparison of two species. Biol. Bull. **182**: 195–209. doi:10.2307/1542113.

Koslow, J.A., Gowlett-Holmes, K., Lowry, J.K., O'Hara, T., Poore, G.C.B., and Williams, A. 2001. Seamount benthic macrofauna off southern Tasmania: community structure and impacts of trawling. Mar. Ecol. Prog. Ser. **213**: 111–125. doi:10.3354/meps213111.

Krieger, K.L., and Wing, B.L. 2002. Megafauna associations with deepwater corals (*Primnoa* spp.) in the Gulf of Alaska. Hydrobiologia, **471**: 83–90. doi:10.1023/A:1016597119297.

Kulka, D.W., and Pitcher, D.A. 2002. Spatial and temporal patterns in trawling activity in the Canadian Atlantic and Pacific. ICES CM 2001/R:02.

Lasker, H.R., Kim, K., and Coffroth, M.A. 1998. Production, settlement, and survival of plexaurid gorgonian recruits. Mar. Ecol. Prog. Ser. **162**: 111–123. doi:10.3354/meps162111.

Levin, I., and Kromer, B. 2004. The tropospheric $^{14}CO_2$ level in mid-latitudes of the northern hemisphere (1959–2003). Radiocarbon, **46**: 1261–1272.

Lewis, J.C., Barnowski, T.F., and Telesnicki, G.J. 1992. Characteristics of carbonates of gorgonian axes. Biol. Bull. **183**: 278–296. doi:10.2307/1542215.

Mills, S.W., and Mullineaux, L.S. 2005. Sizes and distributions of Octocorals *Keratoisis* sp. and *Paragorgia* sp. on the New England Seamount Chain: implications for colonization dynamics. *In* Program and Abstract Book, 3rd International Symposium on Deep-Sea Corals, Miami, Florida, 28 November – 2 December 2005. University of Miami, Rosenstiel School of Marine and Atmospheric Science, Miami, Florida. p. 201.

Mistri, M., and Ceccherelli, V.U. 1994. Growth and secondary production of the Mediterranean gorgonian *Paramuricea clavata*. Mar. Ecol. Prog. Ser. **103**: 291–296. doi:10.3354/meps103291.

Mortensen, P.B., and Buhl-Mortensen, L. 2005. Morphology and growth of the deep-water gorgonians *Primnoa resedaeformis* and *Paragorgia arborea*. Mar. Biol. (Berl.), **147**: 775–788. doi:10.1007/s00227-005-1604-y.

Mortensen, P.B., Buhl-Mortensen, L., and Gordon, D.C., Jr. 2006. Distribution of deep-water corals in Atlantic Canada. *In* Proceedings of the 10th International Coral Reef Symposium, Okinawa, Japan, 28 June – 2 July 2006. Japanese Coral Reef Society, Tokyo, Japan. pp. 1832–1848.

Nydal, R., Brenkert, A.L., and Boden, T.A. 1998. Carbon-14 measurements in surface water CO_2 from the Atlantic, Indian and Pacific Oceans, 1965–1994. Carbon Dioxide Information Analysis Center, Oak Ridge National Laboratory, Oak Ridge, Tennessee. ORNL/CDIAC-104, NDP-057A.

Roark, E.B., Guilderson, T.P., Flood-Page, S., Dunbar, R.B., Ingram, B.L., Fallon, S.J., and McCulloch, M. 2005. Radiocarbon-based ages and growth rates of bamboo corals from the Gulf of Alaska. Geophys. Res. Lett. **32**: L04606. doi:10.1029/2004GL021919.

Roark, E.B., Guilderson, T.P., Dunbar, R.B., and Ingram, B.L. 2006. Radiocarbon-based ages and growth rates of Hawaiian deep-sea corals. Mar. Ecol. Prog. Ser. **327**: 1–14. doi:10.3354/meps327001.

Roberts, J.M., Wheeler, A.J., and Freiwald, A. 2006. Reefs of the deep: the biology and geology of cold-water coral ecosystems. Science (Washington, D.C.), **312**: 543–547. doi:10.1126/science.1119861. PMID:16645087.

Sherwood, O.A., Scott, D.B., Risk, M.J., and Guilderson, T.P. 2005. Radiocarbon evidence for annual growth rings in the deep-sea octocoral *Primnoa resedaeformis*. Mar. Ecol. Prog. Ser. **301**: 129–134. doi:10.3354/meps301129.

Sherwood, O.A., Scott, D.B., and Risk, M.J. 2006. Late Holocene radiocarbon and aspartic acid racemization dating of deep-sea octocorals. Geochim. Cosmochim. Acta, **70**: 2806–2814. doi:10.1016/j.gca.2006.03.011.

Sherwood, O.A., Edinger, E.N., Guilderson, T.P., Ghaleb, B., Risk, M.J., and Scott, D.B. 2008. Late Holocene radiocarbon variability in Northwest Atlantic slope waters. Earth Plan. Sci. Lett. **275**: 146–153. doi:10.1016/j.epsl.2008.08.019.

Stone, R.P. 2006. Coral habitat in the Aleutian Islands: depth distribution, fine-scale species associations, and fisheries implications. Coral Reefs, **25**: 229–238. doi:10.1007/s00338-006-0091-z.

Stuiver, M., and Polach, H.A. 1977. Discussion: reporting of ^{14}C data. Radiocarbon, **19**: 355–363.

Szmant-Froelich, A. 1974. Structure, iodination, and growth of the axial skeletons of *Muricea californica* and *M. fruticosa* (Coelenterata: Gorgonacea). Mar. Biol. (Berl.), **27**: 299–306. doi:10.1007/BF00394365.

Thresher, R.E., Rintoul, S.R., Koslow, J.A., Weidman, C., Adkins, J., and Proctor, C. 2004. Oceanic evidence of climate change in southern Australia over the last three centuries. Geophys. Res. Lett. **31**: L07212. doi:10.1029/2003GL018869.

Thresher, R.E., MacRae, C.M., Wilson, N.C., and Gurney, R. 2007. Environmental effects on the skeletal composition of deep-water gorgonians (*Keratoisis* spp.; Isididae). Bull. Mar. Sci. **81**(3): 409–422.

Tracey, D., Neil, H., Gordon, D., and O'Shea, S. 2003. Chronicles of the deep: ageing deep-sea corals in New Zealand waters. Water and Atmosphere, **11**(2): 22–24.

Tracey, D.M., Neil, H., Marriott, P., Andrews, A.H., Cailliet, G.M., and Sanchez, J.A. 2007. Age and growth of two genera of deep-sea bamboo corals (Family Isididae) in New Zealand waters. Bull. Mar. Sci. **81**(3): 393–408.

Wareham, V.E., and Edinger, E.N. 2007. Distribution of deep-sea coral in the Newfoundland and Labrador Region, Northwest Atlantic Ocean. *In* Conservation and adaptive management of seamount and deep-sea coral ecosystems. *Edited by* R.Y. George and S.D. Cairns. Bull. Mar. Sci. **81**(Suppl. 1): 289–313.

Weidman, C.R., and Jones, G.A. 1993. A shell-derived time history of bomb ^{14}C on Georges Bank and its Labrador Sea implications. J. Geophys. Res. **98**(C8): 14577–14588. doi:10.1029/93JC00785.

Williams, B., Risk, M.J., Ross, S.W., and Sulak, K.J. 2006. Deep-water antipatharians: proxies of environmental change. Geology, **34**(9): 773–776. doi:10.1130/G22685.1.